

Oscillatory dynamics arising from competitive inhibition and multisite phosphorylation

Vijay Chickarmane^{a,*}, Boris N. Kholodenko^b, Herbert M. Sauro^a

^a*Keck Graduate Institute, 535 Watson Dr, Claremont, CA 91711, USA*

^b*Department of Pathology, Anatomy and Cell Biology, Thomas Jefferson University, Philadelphia, Pennsylvania, USA*

Received 7 February 2006; received in revised form 20 April 2006; accepted 19 May 2006

Available online 23 May 2006

Abstract

There have been a growing number of observations of oscillating protein levels (p53 and NFκB) in eukaryotic signalling pathways. This has resulted in a renewed interest in the mechanism by which such oscillations might occur. Recent computational work has shown that a multisite phosphorylation mechanism such as that found in the MAPK cascade can theoretically exhibit bistability. The bistable behavior was shown to arise from sequestration and saturation mechanisms for the enzymes that catalyse the multisite phosphorylation cycle. These effects generate the positive feedback necessary for bistability. In this paper we describe two kinds of oscillatory dynamics which can occur in a network by which, both use such bistable multisite phosphorylated cycles. In the first example, the fully phosphorylated form of the phosphorylated cycle represses the production of the kinase, which carries out the phosphorylation of the unphosphorylated states of the cycle. The dynamics of this system leads to a relaxation oscillator. In the second example, we consider a cascade of two cycles, in which the fully phosphorylated form of the kinase, in the first cycle, phosphorylates the unphosphorylated forms in the second cycle. A feedback loop, by which the fully phosphorylated form of the second cycle inhibits the kinase step in the first cycle is also present. In this case we obtain a ring oscillator. Both these networks illustrate the versatility of the multisite bistable network. © 2006 Elsevier Ltd. All rights reserved.

Keywords: Systems biology; Modelling; MAPK; Phosphorylation; Signalling networks; Bistability; Oscillations

1. Introduction

There have been a growing body of evidence of oscillating protein levels (Hoffmann et al., 2002; Lahav et al., 2004; Wang et al., 2006) in eukaryotic signalling pathways. This has resulted in a renewed interest in the mechanism by which such oscillations might occur.

Arguably one of the most studied protein networks is the MAPK pathway and recent work in Yeast by Wang et al. (2006) has provided evidence for bistability in this pathway which, as we will show in this paper, can be used to generate oscillations. Indeed (Wang et al., 2006) hypothesized that the Yeast pheromone pathway might use bistability to generate oscillations.

What is intriguing about the MAPK pathway in general is that it is replete with feedback loops. One of the first

regulatory loops to be discovered was probably the negative feedback between ERK and SOS (Hu and Bowtell, 1996; Langlois et al., 1995; Cherniack et al., 1995). In addition to the ERK/SOS feedback, a number of other feedback loops have been reported. For example, a second negative feedback arises from hyperphosphorylation of multiple sites on Raf1, which is the first kinase of the MAPK cascade (Dougherty et al., 2005). These sites were shown to be proline-directed targets of activated ERK, and hyperphosphorylation of these sites inhibits the Ras/Raf1 interaction that is necessary for Raf1 activation. A third negative feedback is brought about by ERK-induced inhibitory phosphorylation of the adaptor protein GAB1 (Roshan et al., 1999; Yu et al., 2002; Arnaud et al., 2004; Lehr et al., 2004), which can bind the Grb2-SOS complex and, thereby, participate in Ras activation by growth factors.

In addition to specific regulatory loops there is also less obvious regulation that arises from sequestration effects.

*Corresponding author. Tel.: +1 9096070101.

E-mail address: Vijay_Chickarmane@kgi.edu (V. Chickarmane).

The most well understood of these is one based on the multisite phosphorylation mechanism (Markevich et al., 2004). What is intriguing about this mechanism is that it has the potential to generate bistability and oscillations.

The MAPK pathway serves as one example where many regulatory loops have been uncovered, other protein networks are equally adorned with similar interactions (Ihekweaba et al., 2005; Bond et al., 2005) and many more undoubtedly remain to be uncovered. These interactions have the potential to generate a great variety of dynamical behaviors as witnessed by recent experimental work on single cells (Kaern and Weiss, 2006). In many cases, however, it is difficult to understand the origin of these observations because this requires a knowledge of motifs and their dynamical properties. In many cases experimentalists rely on published theoretical models to compare to real networks (cf. Wang et al., 2006).

In this paper we wish to explore a number of novel motifs that can elicit oscillatory behavior. Thus, although the networks that we will describe are hypothetical, they serve their purpose to the community by suggesting possible ways in which observed data can be explained. We will be particularly interested in motifs where the regulatory interactions are coupled with dual-phosphorylation cycles (Fig. 1).

We begin by briefly reviewing the bistable switch-like model of Markevich et al. (2004) in Section 2. In Section 3,

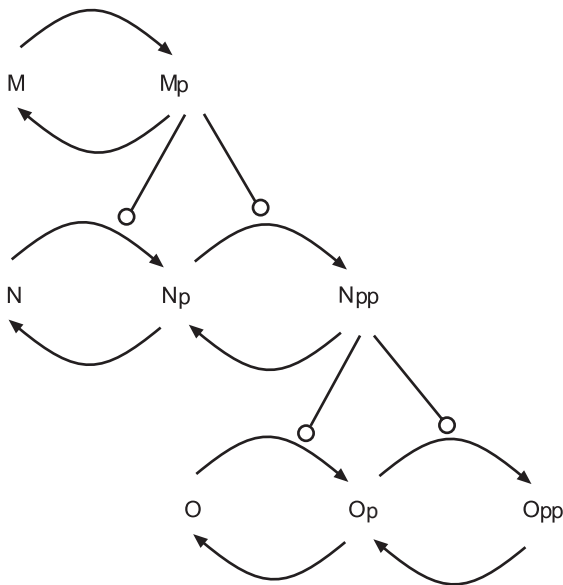


Fig. 1. MAPK Modular structure: hierarchical three-tiered structure for a typical MAPK module. The symbol X , X_p and X_{pp} represent the unphosphorylated, single phosphorylated and doubly phosphorylated forms. Each layer designates a distinct protein species, the first layer, populated with protein species M , is only singly phosphorylated, the two lower layers, populated by species N and O and doubly phosphorylated. In each layer, forward reactions are catalysed by kinases and reverse reactions by phosphatases. Each forward arm consumes ATP (with the release of ADP) and each reverse arm releases free phosphate. The kinase activities in layers N and O are provided by the phosphorylated forms in the previous layer.

we construct a relaxation oscillator by assuming that the fully phosphorylated form of the kinase in the cycle represses the production of its upstream phosphorylating kinase. In Section 4 we construct a ring oscillator made from two cascade layers in which the fully phosphorylated form of the kinase in the first layer activates the second, and a feedback loop in which the fully phosphorylated form of the second layer competitively binds to the kinase which phosphorylates the first layer.

1.1. Methods

All simulations were carried out using the Systems Biology Workbench (SBW/BioSPICE) tools (Sauro et al., 2003): the network designer, JDesigner, and the simulation tool Jarnac (Sauro, 2000). Bifurcation diagrams were computed using SBW with an interface to MATLAB (Wellock et al., 2005), and a bifurcation discovery tool (Chickarmane et al., 2005). Bifurcation plots were also computed and confirmed using Oscill8,¹ an interactive bifurcation software package developed by Emery Conrad, which is linked to AUTO (Doedel, 1981), and SBW (Sauro et al., 2003). In all our simulations the species concentrations are regarded as dimensionless, whereas the kinetic constants have dimensions of inverse time, with dimensionless Michaelis–Menten constants. All models are available as standard SBML or Jarnac scripts (<http://www.sys-bio.org>).

2. Bistable switch due to multisite phosphorylation

In Markevich et al. (2004), the authors described a kinetic scheme where a two-site covalent-modification cycle, of a substrate M , is acted upon by a phosphatase (Phos) and a kinase (Kin), both in a non-processive, distributive way, such that the activity of M , showed bistability. Fig. 2 shows the reaction scheme of a dual-phosphorylation subnetwork, with three states of increasing phosphorylation, M , M_p , M_{pp} . All the arrows represent reactions governed by Michaelis–Menten kinetics.

The model assumes that the phosphorylation steps are irreversible while the dephosphorylation steps are irreversible and product sensitive. This scheme results in the sequestration of Phos, by its products, M_p and M . The sequestration of modifying enzymes effectively adds inhibitory loops into the network (Fig. 3). The first inhibition occurs when M suppresses the dephosphorylation of M_p . The second inhibition occurs when M_{pp} suppresses the dephosphorylation of M_p which occurs because M_{pp} sequesters Phos, thereby reducing its availability to M_p . These interactions lead to a positive feedback loop that stimulates the production of M_{pp} . The physical explanation for this is as follows. Increasing the kinase activity on v_1 and v_2 (Fig. 3) results in additional production of M_{pp} . The additional M_{pp} sequesters

¹<http://sourceforge.net/projects/oscill8>.

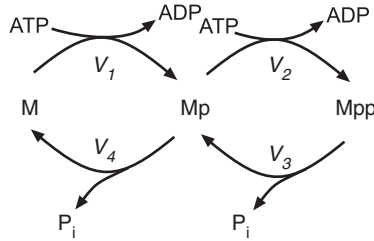


Fig. 2. Dual-phosphorylation scheme: the diagram shows the reaction scheme for the multisite phosphorylation. Phosphorylation is carried out by the forward reactions, whereas the dephosphorylation is carried out by the reverse reactions.

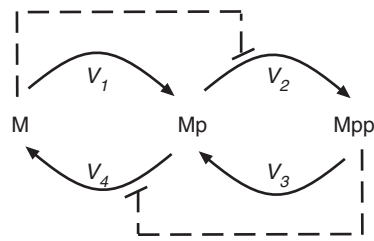


Fig. 3. Implied regulation: this is the same network as shown in Fig. 2 but with some of the implied regulatory feedback loops added as a result of sequestration effects. M suppresses the phosphorylation of M_{pp} , whereas M_{pp} suppresses the dephosphorylation of M_p .

phosphatase which means that M_p is not consumed as fast and tends to rise. By conservation this must result in a decline in M . The increase in M_p stimulates further increases in M_{pp} which thereby creates the positive feedback. The increase in M_{pp} is further ensured by making sure that the M_{pp} phosphatase is near saturation, thus preventing the additional M_{pp} being dissipated by dephosphorylation. In addition, the rise in M_p is also enhanced by making sure that the Kinase (v_1) with respect to M is close to saturation. These factors together result in bistability.

We briefly review the model given in Markevich et al. (2004), so that the results can be used to construct the networks we discuss later in the text. The equations for the species M , M_p and M_{pp} are assumed to be described by Michaelis–Menten equations. The mass-balance equations are given by

$$\frac{dM}{dt} = v_4 - v_1,$$

$$\frac{dM_{pp}}{dt} = v_2 - v_3,$$

$$\frac{dM_p}{dt} = -\left(\frac{dM}{dt} + \frac{dM_{pp}}{dt}\right), \quad (1)$$

where the last equation reflects the conservation of mass, $M_t = M + M_p + M_{pp}$. v_1, v_2, v_3, v_4 , are the reaction rates described by the kinetics laws

$$v_1 = \frac{k_1^{cat}(\text{Kin}/Km_1)M}{1 + M_p/Km_2 + M/Km_1},$$

$$v_2 = \frac{k_2^{cat}(\text{Kin}/Km_2)M_p}{1 + M_p/Km_2 + M/Km_1},$$

$$v_3 = \frac{k_3^{cat}(\text{Phos}/Km_3)M_{pp}}{1 + M_{pp}/Km_3 + M_p/Km_4 + M/Km_5},$$

$$v_4 = \frac{k_4^{cat}(\text{Phos}/Km_4)M_p}{1 + M_{pp}/Km_3 + M_p/Km_4 + M/Km_5}. \quad (2)$$

The kinetic constants are the same as in Markevich et al. (2004), and are given below in Table 1.

Note the form of the denominator in the equations for v_3 and v_4 , it includes terms for all three substrates, M , M_p and M_{pp} . This represents the competition for the phosphatase by the three substrates. In the appendix, we derive the following simple expression which relates M_p to M_{pp} and M ,

$$M_p^2 = \frac{k_1^{cat}k_3^{cat}Km_2Km_4}{k_2^{cat}k_4^{cat}Km_1Km_3} MM_{pp}. \quad (3)$$

Using the conservation equation, we can eliminate M_p , and obtain a quadratic equation for M_{pp} , in terms of M

$$(M_t - M_{pp} - M)^2 = \alpha MM_{pp}, \quad (4)$$

where

$$\alpha = \frac{k_1^{cat}k_3^{cat}Km_2Km_4}{k_2^{cat}k_4^{cat}Km_1Km_3}.$$

We choose one of the two roots, and using Eqs. (1) and (2), express M_{pp} as a function of Kin. In Fig. 4, we plot this dependence, which shows the bistable behavior of M_{pp} with respect to Kin.

Using the bistable behavior of the cascade, we now construct two types of networks which can exhibit oscillations, a relaxation oscillator and a ring oscillator.

3. Oscillator type 1: relaxation oscillator

The relaxation oscillator is a commonly used device in engineering for generating oscillatory non-sinusoidal signals, such as square or sawtooth waves. It is a device that repeatedly alternates between two states with a period that depends on a charging mechanism coupled to a threshold device. In electronic devices the charging is usually carried out by a capacitor or an inductor and the threshold device is often a transistor or even a simple neon lamp. However, relaxation oscillators are not confined to man-made devices, biological relaxation oscillators are also known. Probably, the most famous example of a biological relaxation oscillator is a model based on a simplification of the Hodgkin–Huxley equations for modelling nerve action potentials. More recently, Hasty et al. (2002) described the synthetic construction of a relaxation oscillator to induce synchronous oscillations. In biological relaxation oscillators, the threshold device can be a simple bistable switch and the ‘‘charging capacitor’’ the rise and fall of a protein species. The protein species is ‘‘charged’’

Table 1
Parameter values for the Markevich bistable model

k_1^{cat}	k_2^{cat}	k_3^{cat}	k_4^{cat}	Km_1	Km_2	Km_3	Km_4	Km_5	Phos	M_t
0.01	15	0.06	0.084	50	500	22	18	86	100	500

The level of Kin is omitted from the table because it varies during the simulations. Values for Kin ranging from roughly 45 to 60 units lead to bistability (see Fig. 4).

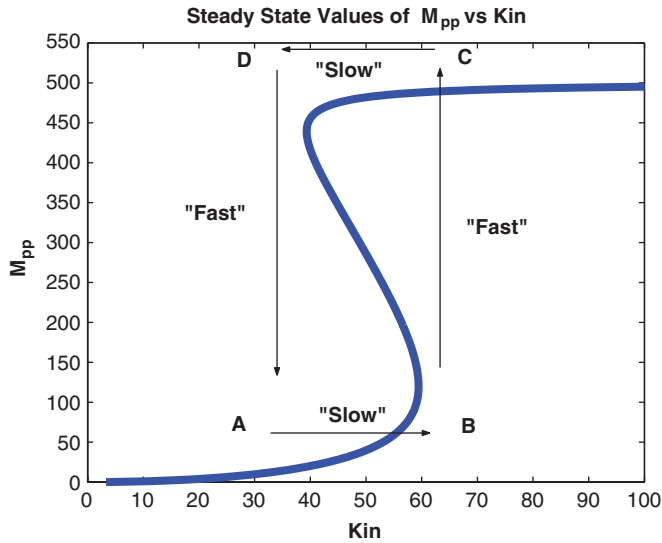


Fig. 4. Bistability in a dual-phosphorylation scheme: the steady-state values of M_{pp} as a function of Kin, which shows bistable switch-like behavior. The graph also illustrates the two time-scales in bistable dynamics, one fast that occurs during the switching action and a slow dynamic due to the discharge mechanism.

by the bistable switch when in the on state but upon reaching a set concentration the protein switches the bistable switch to the off state. A protein degradation step ensures the discharge of the protein so that eventually it switches the bistable switch back to its on state, and thus the cycle continues. Fig. 5 shows a schematic for a biological relaxation oscillator.

In this section we describe the design of a relaxation oscillator based on a protein kinase/phosphatase network. The reviews by Tyson et al. (2003) and Kholodenko (2006) illustrate a number of different oscillators, including relaxation oscillators and are a useful reference to consult for more information.

Consider a scheme where the production of Kin is affected by the fully phosphorylated form of M , i.e. M_{pp} . We will assume that the equation governing the dynamics of Kin is given by

$$\frac{dKin}{dt} = \frac{\alpha}{1 + M_{pp}/K} - \gamma Kin, \quad (5)$$

where the negative feedback loop due to M_{pp} , has the effect of reducing the production of Kin. The equation is not based on any experimental observations of feedback mechanisms but is used to illustrate one possible way to

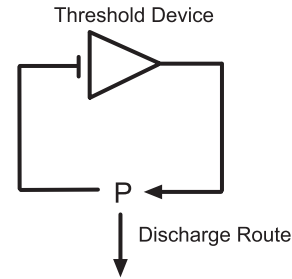


Fig. 5. Relaxation oscillator: the diagram shows a schematic for a general relaxation oscillator. The mechanism depends on two features, a threshold device which can activate and deactivate according to a graded input and a discharge device (P) which can charge when the threshold device is active and discharge when inactive. In a biological system, the charging device can be a simple protein activation step, with the discharge being coupled with deactivation. The threshold device can be a bistable system. The discharge device also provides the necessary delay. Note that the input to the threshold device is inverted.

generate a feedback response in a protein network. The input to the system, Kin, is coupled to the output M_{pp} , through Eq. (5). In Fig. 6 we show the reaction network, which shows M_{pp} acting as an inhibitor of Kin production.

In Fig. 4, we follow the bistable curve along the path A–D. At point A, Kin is at a low level, and it initiates the phosphorylation of M , and hence the M_{pp} levels begin to slowly increase. On reaching point B, the system jumps to C. At C all of the protein is phosphorylated, and M_{pp} is at its highest value. At this point (see Eq. (5)), the Kin levels drop drastically, since M_{pp} has the effect of suppressing Kin. This in turn stops the further phosphorylation of M , and hence moves the system from C to D, at which point there is another sudden jump, in which the final levels of Kin and M_{pp} are low, and the system is back to its starting point A. This completes one complete cycle of oscillation. The parameters for the bistable switch are known (Markevich et al., 2004), hence the only unknowns are the parameters in Eq. (5), which are determined by computing the conditions for which the Hopf bifurcation occurs. At the Hopf bifurcation, for a complex pair of eigenvalues of the Jacobian matrix, the positive real parts cross the imaginary axis, becoming positive, signalling the onset of an instability. In the appendix we derive the necessary conditions for a Hopf bifurcation, which leads to the following equation:

$$f1 = (HFA + BDI - AEI - CDH) + (AE + AI + EI - HF - BD)(I + A + E) = 0. \quad (6)$$

At a Hopf bifurcation the parameters α , γ and K , have to be chosen such that the above condition is satisfied, as well as $\rho^2 = (AE + AI + EI - HF - BD) \geq 0$. Using Eq. (5), the steady-state value of M_{pp} as a function of K_{in} can be computed. Using optimization methods such as gradient descent, we solve these simultaneous nonlinear equations. The solutions of these nonlinear equations allow us to map regions in the three-dimensional space, at which oscillations occur.

The above set of equations allow us to select the following parameters, $\alpha = 0.1$, $\gamma = 10^{-4}$, and $K = 10$, for which oscillations occur. For this particular choice, Fig. 7A shows time series plots for M , M_p , M_{pp} and K_{in} . The plots show M and M_{pp} oscillate with large amplitudes, exchanging mass with each other, whereas M_p barely changes. M_p forms a bridge between the unphosphorylated and fully phosphorylated forms of M . Fig. 7B shows the bifurcation plot, of the steady states of M_{pp} and shows a supercritical and subcritical Hopf bifurcation at two values of the degradation rate of K_{in} , i.e. γ . Within the oscillatory region, i.e. $5.6 \times 10^{-5} < \gamma < 1.22 \times 10^{-4}$, the amplitude of oscillations are approximately constant.

4. Oscillator type 2: ring oscillator

The previous model illustrated a particular kind of oscillator called the relaxation oscillator. The advantage of

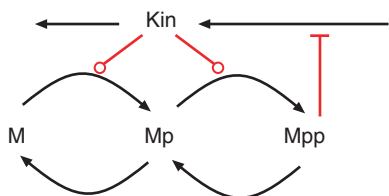


Fig. 6. Relaxation oscillator: the diagram shows the reaction scheme for a relaxation oscillator based on a dual-phosphorylation scheme. The negative feedback from M_{pp} provides a route to the discharge circuit (Kin). Bistability is provided by the dual-phosphorylation scheme which is controlled by Kin.

a relaxation oscillator is the small number of independent molecular species that are required to make it operate (two at minimum). Other kinds of oscillators also exist, most notably the feedback oscillator, however these require more independent species to function. The feedback oscillator is well understood in the engineering community and many examples have been studied in biology (e.g. Higgins, 1967; Tyson and Othmer, 1978).

A related type of oscillator to the relaxation oscillator is the ring oscillator. Whereas a relaxation oscillator is made of a charging and a threshold device, the ring oscillator is made from a series of threshold devices that form a ring. Each threshold device is used to switch the next unit to the opposite state, as a result, ring oscillators require an odd number of cascade units.

Previous work (Sauro, 1993; Gonze and Goldbeter, 2001; Elowitz and Leibler, 2000) on ring oscillators have exploited ultrasensitivity to provide the threshold mechanism between the switching units. Here we construct a ring oscillator based on two bistable switches and a negative feedback. Clearly, the greater the number of cascades, the greater the delay, and hence the more effective the negative feedback is in producing oscillations. In the multisite phosphorylation mechanism we consider, each kinase cascade is itself a bistable switch, and hence in principle one could have two switches connected in series, with a negative feedback, between the output of the second switch and the input, which could produce oscillations. In Fig. 8, we plot a cartoon of the scheme that we have just described.

The equations for the reactions are given below:

$$\frac{dM}{dt} = v_4 - v_1,$$

$$\frac{dM_{pp}}{dt} = v_2 - v_3,$$

$$\frac{dM_p}{dt} = -\left(\frac{dM}{dt} + \frac{dM_{pp}}{dt}\right),$$

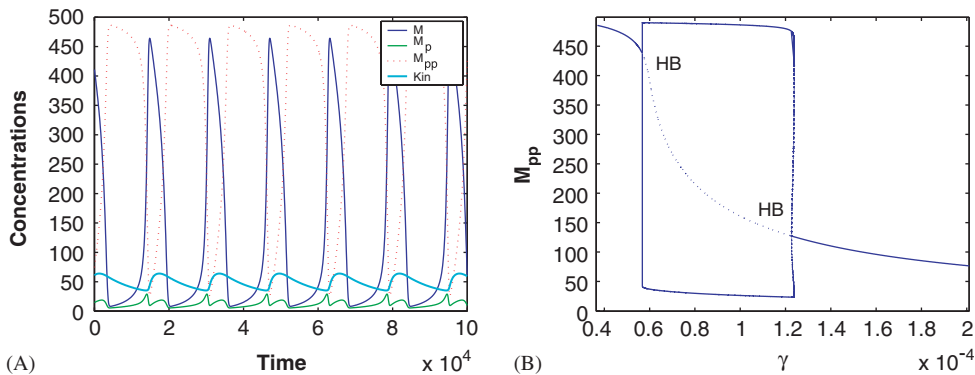


Fig. 7. Time series plots for the relaxation oscillator: in (A) we show time series plots for M , M_p , M_{pp} and K_{in} for the parameters $\alpha = 0.1$, $\gamma = 10^{-4}$, and $K = 10$. In (B) we plot the bifurcation diagram for the steady-state values of M_{pp} , with respect to γ . There are two Hopf bifurcation points (marked by symbol HB), where the first is supercritical and the second is subcritical.

$$\begin{aligned} \frac{dN}{dt} &= v_8 - v_5, \\ \frac{dN_{pp}}{dt} &= v_6 - v_7, \\ \frac{dN_p}{dt} &= -\left(\frac{dN}{dt} + \frac{dN_{pp}}{dt}\right), \\ \frac{dKin}{dt} &= \alpha_0 - \gamma_0 Kin, \end{aligned} \quad (7)$$

where $v_1 - v_8$, the reaction rates are described by

$$\begin{aligned} v_1 &= \frac{k_1^{cat}(Kin/Km_1)M}{1 + M_p/Km_2 + M/Km_1} \left[\frac{1}{1 + N_{pp}/K_I} \right], \\ v_2 &= \frac{k_2^{cat}(Kin/Km_2)M_p}{1 + M_p/Km_2 + M/Km_1} \left[\frac{1}{1 + N_{pp}/K_I} \right], \\ v_3 &= \frac{k_3^{cat}(Phos_1/Km_3)M_{pp}}{1 + M_{pp}/Km_3 + M_p/Km_4 + M/Km_5}, \\ v_4 &= \frac{k_4^{cat}(Phos_2/Km_4)M_p}{1 + M_{pp}/Km_3 + M_p/Km_4 + M/Km_5}, \\ v_5 &= \frac{k_5^{cat}(M_{pp}/Km_1)N}{1 + N_p/Km_2 + N/Km_1}, \end{aligned}$$

$$\begin{aligned} v_6 &= \frac{k_6^{cat}(M_{pp}/Km_2)N_p}{1 + N_p/Km_2 + N/Km_1}, \\ v_7 &= \frac{k_7^{cat}(Phos_2/Km_3)N_{pp}}{1 + N_{pp}/Km_3 + N_p/Km_4 + N/Km_5}, \\ v_8 &= \frac{k_8^{cat}(Phos_2/Km_4)N_p}{1 + N_{pp}/Km_3 + N_p/Km_4 + N/Km_5}. \end{aligned} \quad (8)$$

Table 2 includes the additional rate constants for this model. The other rates constants are the same as given in Table 1.

The form of the feedback from N_{pp} suggests that there is competition between N_{pp} and the unphosphorylated forms of the first kinase, M, M_p to bind to Kin. N_{pp} sequesters Kin and reduces its availability to the first kinase, thereby providing a negative feedback. An analytical formula for the conditions under which the above system undergoes limit cycle oscillations is fairly complicated, and hence will not be described here. Instead, we performed a bifurcation analysis of the steady states of the network with respect to K_I , the parameter which encodes the feedback strength. The analysis led to regions in parameter space for which the system oscillates. In Fig. 9A, we show the results of the bifurcation analysis, which shows a Hopf bifurcation at $K_I \simeq 66$.

Using this plot, we fix the parameter $K_I = 100$, and plot the time series of M_{pp}, N_{pp} , and Kin. See Fig. 9B. The time series plots for M, N , are phase shifted and are approximately of the same magnitude as M_{pp}, N_{pp} , and M_p, N_p , are small and similar to M_p as was described for the single cascade case. From the figure, we notice that as M_{pp} starts to increase, the second kinase gets phosphorylated, and makes N_{pp} switch to a high level. This in turn sequesters Kin, and ultimately switches OFF, M_{pp} . This then decreases the phosphorylation of N , which switches OFF N_{pp} . Completing the loop, this results in a release of the sequestered Kin, which therefore restarts the phosphorylation of M . The series of two cascades and a negative feedback can be pictured as two switches connected in series, closing the loop with a NOT gate, Fig. 8B. We assume that the degree of sequestration is small compared to the total amount of M .

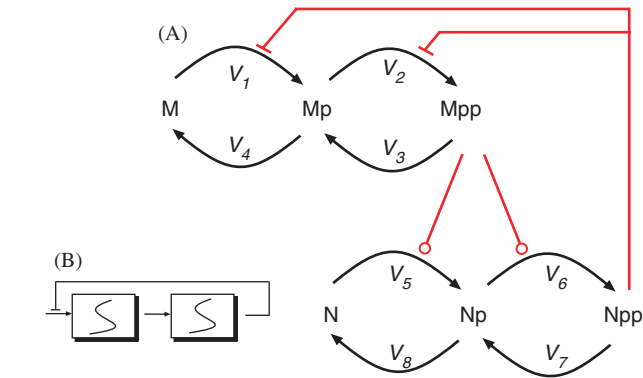


Fig. 8. Ring oscillator: panel (A) shows the reaction scheme for the ring oscillator, comprising of two dual-phosphorylation layers, in which the second layer feeds a negative feedback to the input of the first. Phosphorylation is assumed to be provided by consumption of ATP with the release of ADP. It is assumed that the phosphatases release free phosphate. Panel (B) shows a high level diagram of the ring oscillator, comprising of two bistable stable circuits connected by a negative feedback. Inhibition of V_1 and V_2 is brought about by competition between the cycle components (M and M_p) and N_{pp} which bind to the input kinase.

5. Conclusions

Previous computational work (Markevich et al., 2004) has shown that bistable behavior can arise from sequestration of enzymes that catalyse multisite phosphorylation

Table 2
Additional parameters for the ring oscillator, other parameters are given in Table 1

α_0	γ_0	k_5^{cat}	k_6^{cat}	k_7^{cat}	k_8^{cat}	Phos ₁	Phos ₂	K_I	M_t	N_t
0.8	0.006	2.5×10^{-3}	3.75	0.084	0.06	100	100	100	500	500

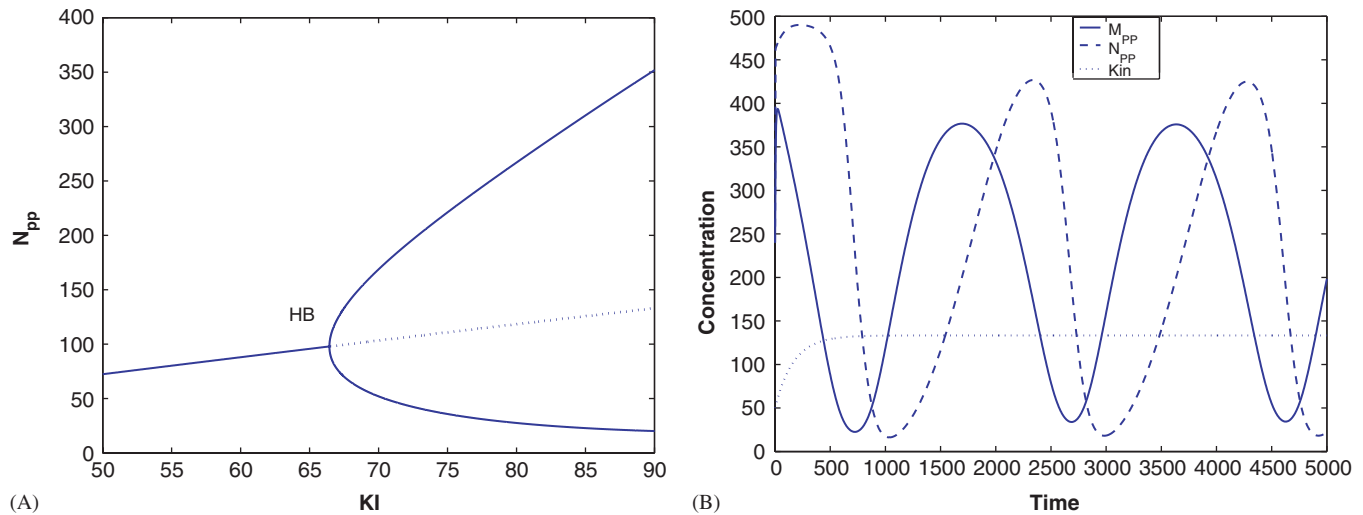


Fig. 9. Bifurcation diagram for the ring oscillator: in panel (A) we plot the bifurcation diagram for the steady-state values of N_{pp} , with respect to K_I . There is a Hopf bifurcation point, at $K_I \simeq 66$. In panel (B) we show time series plots for M_{pp} , N_{pp} and K_{in} for the parameter $K_I = 100$.

cycles. This in turn can generate the positive feedback necessary for bistability. Recent work by Wang et al. (2006) has provided experimental evidence to support this kind of mechanism. In this paper we discuss two oscillatory motifs that can be constructed from the Markevich switch (Markevich et al., 2004) using feedback. These motifs include a relaxation oscillator and the related ring oscillator, both can be seen in Figs. 6 and 8. Previous models (Kholodenko, 2000) have used three layers to generate oscillation. We demonstrate that at a minimum, an oscillatory network can be constructed from a single dual-phosphorylated cycle coupled with a feedback. This is achieved by inhibiting the production of the input kinase by feeding back the fully phosphorylated form of the cycle to the input kinase. This motif leads to a relaxation oscillator. A relaxation oscillator exhibits conspicuous dynamics, in that there are two time-scales involved: one is related to a slow charging process, and the other to the rapid threshold switch. In the second example, we consider two layers, in which the fully phosphorylated form of the first layer is an input kinase to the second layer. In this way a single bistable switch is coupled to another bistable switch. In addition, a feedback from the fully phosphorylated form of the second layer is assumed to inhibit the phosphorylation of the first layer by the input kinase. In this case we obtain a ring oscillator, which functions somewhat differently from the relaxation oscillator. The temporal profiles are quite different in these two cases discussed, and this is one way to differentiate the underlying dynamics.

In addition to the two models we describe here, the paper by Wang et al. (2006) describes an additional motif that can oscillate. The motif they describe is a classic relaxation oscillator which uses the synthesis and degradation of the unphosphorylated protein to generate the charging mechanism and the bistable switch to provide the threshold device.

One of the main issues facing experimental systems biology is reconciling complex network patterns and function. The experimental work described by Wang et al. (2006) is an illustration of the importance of understanding specific motifs using theoretical models and how theory can illuminate function. Many of the advances in our understanding of network function stems from our ability to map theoretical studies onto experimentally derived network diagrams. This process is hindered by our limited knowledge of motif properties. In this paper we describe two new motifs structures which can be added to a growing list of known theoretical motifs. Our own aim in this work is to build a library of motifs that can be used to assist experimentalists in identifying particular network configurations and thus dynamical function. A good example of such a library can be found in the recent review by Kholodenko (2006) which describes a great variety of motif patterns.

Acknowledgments

This work was supported by grants from the National Science Foundation (0432190 and FIBR 0527023 to H.M.S). V. C and H.M. S are grateful for generous support from DARPA/IPTO BioComp program, contract number MIPR 03-M296-01. B.N. K is grateful to support from the National Institute of Health Grant GM59570.

Appendix

In this appendix, we provide detailed derivations for Eq. (3), and the linear stability analysis leading to Eq. (6). The steady-state values for M and M_{pp} are obtained by setting the time derivatives in Eq. (1) to zero, i.e. $v_4 = v_1$ and $v_2 = v_3$. We use Eq. (2) for the rates v_1, v_2, v_3 and v_4 , to obtain, for $v_4 = v_1$,

$$\frac{1 + M_p/Km_2 + M/Km_1}{1 + M_{pp}/Km_3 + M_p/Km_4 + M/Km_5} = \frac{k_1^{cat} M(Kin/Km_1)}{k_4^{cat} M_p(Phos/Km_4)}, \quad (9)$$

and for $v_2 = v_3$

$$\frac{1 + M_p/Km_2 + M/Km_1}{1 + M_{pp}/Km_3 + M_p/Km_4 + M/Km_5} = \frac{k_2^{cat} M(Kin/Km_2)}{k_3^{cat} M_{pp}(Phos/Km_4)M_{pp}}. \quad (10)$$

Equating the above two equations we obtain Eq. (3) in the main text

$$\frac{k_1^{cat} k_3^{cat} M K m_4}{k_2^{cat} k_4^{cat} M_p K m_1} = \frac{M_p K m_3}{M_{pp} K m_2}. \quad (11)$$

Linear stability analysis: We now present a linear stability analysis of Eqs. (2) and (3), from which we can derive the condition, Eq. (6). We first linearize Eqs. (2) and (3) and compute the Jacobian, which takes the following form, with the independent variables being M , M_{pp} and Kin :

$$J = \begin{bmatrix} \frac{\partial(V4 - V1)}{\partial M} & \frac{\partial(V4 - V1)}{\partial M_{pp}} & \frac{\partial(V4 - V1)}{\partial Kin} \\ \frac{\partial(V2 - V3)}{\partial M} & \frac{\partial(V2 - V3)}{\partial M_{pp}} & \frac{\partial(V2 - V3)}{\partial Kin} \\ 0 & \frac{-\alpha/K}{(1 + M_{pp}/K)^2} & -\gamma \end{bmatrix} = \begin{bmatrix} A & B & C \\ D & E & F \\ 0 & H & I \end{bmatrix}. \quad (12)$$

The eigenvalues are obtained by solving for the characteristic equation, which leads to, $det(J - \lambda Id) = 0$. At a Hopf bifurcation, one of the eigenvalues is real, $-s$ and there exist a pair of imaginary eigenvalues $\pm i\rho$, and hence the characteristic equation takes the form

$$(\lambda^2 + \rho^2)(\lambda + s). \quad (13)$$

Comparing this simple expression with the characteristic equation that is obtained from Eq. (12) we get, expressions for the eigenvalues

$$s = -(I + A + E),$$

$$\rho^2 = (AE + AI + EI - HF - BD),$$

$$s\rho^2 = (HFA + BDI - AEI - CDH). \quad (14)$$

From the above, we obtain

$$f1 = (HFA + BDI - AEI - CDH) + (AE + AI + EI - HF - BD)(I + A + E) = 0. \quad (15)$$

References

- Arnaud, M., Crouin, C., Deon, C., Loyaux, D., Bertoglio, J., 2004. Phosphorylation of grb2-associated binder 2 on serine 623 by erk mapk regulates its association with the phosphatase shp-2 and decreases stat5 activation. *J. Immunol.* 173, 3962–3971.
- Bond, G.L., Hu, W., Levine, A.J., 2005. Mdm2 is a central node in the p53 pathway: 12 years and counting. *Curr. Cancer Drug Targets* 5, 3–8.
- Cherniack, A.D., Klarlund, J.K., Conway, B.R., Czech, M.P., 1995. Disassembly of son-of-sevenless proteins from grb2 during p21ras desensitization by insulin. *J. Biol. Chem.* 270, 1485–1488.
- Chickarmane, V., Paladugu, S.R., Bergmann, F., Sauro, H.M., 2005. Bifurcation discovery tool. *Bioinformatics* 21 (18), 3688–3690.
- Doedel, E.J., 1981. Auto: a program for the automatic bifurcation analysis of autonomous systems. In: *Proceedings of the Manitoba Conference on Numerical Mathematics and Computation*, 10th, Winnipeg, Canada (Congressus Numeratum 30, 265–284).
- Dougherty, M.K., Muller, J., Ritt, D.A., Zhou, M., Zhou, X.Z., Copeland, T.D., Conrads, T.P., Veenstra, T.D., Lu, K.P., Morrison, D.K., 2005. Regulation of raf-1 by direct feedback phosphorylation. *Mol. Cell.* 17, 215–224.
- Elowitz, M.B., Leibler, S., 2000. A synthetic oscillatory network of transcriptional regulators. *Nature* 403, 335–338.
- Gonze, D., Goldbeter, A., 2001. A model for a network of phosphorylation–dephosphorylation cycles displaying the dynamics of dominoes and clocks. *J. Theor. Biol.* 210, 167–186.
- Hasty, J., McMillen, D., Collins, J.J., 2002. Engineered gene circuits. *Nature* 420, 224–230.
- Higgins, J., 1967. The theory of oscillating reactions. *Ind. Eng. Chem.* 59 (5), 18–62.
- Hoffmann, A., Levchenko, A., Scott, M.L., Baltimore, D., 2002. The IkappaB-NF-kappaB signaling module: temporal control and selective gene activation. *Science* 298, 1241–1245.
- Hu, Y., Bowtell, D.D., 1996. Sos1 rapidly associates with grb2 and is hypophosphorylated when complexed with the egf receptor after egf stimulation. *Oncogene* 12, 1865–1872.
- Ihekwa, A.E.C., Broomhead, D.S., Grimley, R., Benson, N., White, M.R.H., Kell, D.B., 2005. Synergistic control of oscillations in the nf-kb signalling pathway. *IEE Proc.-Syst. Biol.* 152, 153–160.
- Kaern, M., Weiss, R., 2006. Synthetic gene regulatory systems. In: Szallasi, Z., Stelling, J., Periw, V. (Eds.), *System Modeling in Cellular Biology*. MIT Press, Cambridge, MA, pp. 269–295.
- Kholodenko, B.N., 2000. Negative feedback and ultrasensitivity can bring about oscillations in the mitogen-activated protein kinase cascades. *Eur. J. Biochem.* 267, 1583–1588.
- Kholodenko, B.N., 2006. Cell-signalling dynamics in time and space. *Nat. Rev. Mol. Cell. Biol.* 7, 165–176.
- Lahav, G., Rosenfeld, N., Sigal, A., Geva-Zatorsky, N., Levine, A.J., Elowitz, M.B., Alon, U., 2004. Dynamics of the p53-mdm2 feedback loop in individual cells. *Nature, Genetics* 36 (2), 147–150.
- Langlois, W.J., Sasaoka, T., Saltiel, A.R., Olefsky, J.M., 1995. Negative feedback regulation and desensitization of insulin- and epidermal growth factor-stimulated p21ras activation. *J. Biol. Chem.* 270, 25320–25323.
- Lehr, S., Kotzka, J., Avci, H., Sickmann, A., Meyer, H.E.A., Herkner, D.M.-W., 2004. Identification of major erk-related phosphorylation sites in gab1. *Biochemistry* 43, 12133–12140.
- Markevich, N.I., Hoek, J.B., Kholodenko, B.N., 2004. Signaling switches and bistability arising from multisite phosphorylation in protein kinase cascades. *J. Cell Biol.* 164, 353–359.
- Roshan, B., Kjelsberg, C., Spokes, K., Eldred, A., Crovello, C.S., Cantley, L.G., 1999. Activated erk2 interacts with and phosphorylates the docking protein gab1. *J. Biol. Chem.* 274, 36362–36368.
- Sauro, H.M., 1993. A biochemical nand gate and assorted circuits. In: Schuster, S., Rigoulet, M., Ouhabi, R., Mazat, J.-P. (Eds.), *Modern Trends in Biothermokinetics*. Plenum Press, New York, London, pp. 133–140.

- Sauro, H.M., 2000. Jarnac: a system for interactive metabolic analysis. In: Hofmeyr, J.-H.S., Rohwer, J.M., Snoep, J.L. (Eds.), *Animating the Cellular Map: Proceedings of the Ninth International Meeting on BioThermoKinetics*. Stellenbosch University Press.
- Sauro, H.M., Hucka, M., Finney, A., Wellock, C., Bolouri, H., Doyle, J., Kitano, H., 2003. Next generation simulation tools: the systems biology workbench and biospice integration. *OMICS* 7 (4), 355–372.
- Tyson, J., Othmer, H.G., 1978. The dynamics of feedback control circuits in biochemical pathways. In: Rosen, R., Snell, F.M. (Eds.), *Progress in Theoretical Biology*, vol. 5, pp. 1–62.
- Tyson, J.J., Chen, K.C., Novak, B., 2003. Sniffers, buzzers, toggles and blinkers: dynamics of regulatory and signaling pathways in the cell. *Curr. Opin. Cell Biol.* 15, 221–231.
- Wang, X., Hao, N., Dohlman, H., Elston, T.C., 2006. Computational and experimental analysis of bistability, stochasticity and oscillations in the mitogen activated protein kinase cascade. *Biophys. J.* 90, 1961–1978.
- Wellock, C., Chickarmane, V., Sauro, H.M., 2005. The sbw-matlab interface. *Bioinformatics* 21, 823–824.
- Yu, C.F., Liu, Z.X., Cantley, L.G., 2002. Erk negatively regulates the epidermal growth factor-mediated interaction of *gab1* and the phosphatidylinositol 3-kinase. *J. Biol. Chem.* 277, 19382–19388.